

Structure–reactivity relationships in a recognition mediated [3+2] dipolar cycloaddition reaction†

Andrew J. Sinclair, Vicente del Amo and Douglas Philp*

Received 23rd April 2009, Accepted 13th May 2009

First published as an Advance Article on the web 23rd June 2009

DOI: 10.1039/b908072d

The [3+2] dipolar cycloaddition between an azide and maleimide can be accelerated by a factor of more than 100 simply by attaching complementary recognition sites to the reactive partners. This rate acceleration derives from the formation of a reactive binary complex between the azide and the maleimide. The variation of the observed rate acceleration with simple structural changes, such as adding additional rotors, should be relatively predictable. However, the application of a simple, rotor-based increment in the systems reported here is insufficient to predict reactivity correctly. Computational studies suggest that the nature of the available reaction pathways within the binary complex formed by the reactants is important in determining the reactivity of a given complex.

Introduction

A key objective of supramolecular chemistry is the use of molecular recognition to achieve the acceleration¹ and control² of chemical reactions. As part of our program³ on the study of self-replicating systems, we have been exploring the consequences of recognition processes on the acceleration of solution phase Diels–Alder⁴ and [3+2] dipolar⁵ cycloaddition reactions. In previous examples, we have demonstrated that the location of complementary recognition sites on the components of a [3+2] dipolar cycloaddition, namely dipole **A** and dipolarophile **B**, allows the association of these reactive partners in a binary complex [**A**·**B**]. If, as a result of formation of this complex, the reactive groups are then oriented in a mutually suitable geometry, the reaction is rendered *pseudo*-intramolecular within the [**A**·**B**] complex. It is therefore expected that some of the unfavourable entropic cost of organising the reactive partners is shifted to the binding event earlier in the reactive sequence and it is reasonable to expect⁶ that the formation of the [**A**·**B**] complex will effect significant rate acceleration. In order to apply this concept to the transition metal-free⁷ [3+2] dipolar cycloadditions of azides, we designed the azide dipole **1a** based on an amidopicoline moiety, and the maleimide dipolarophiles **2a**, **3a** and **4a**, based on a carboxylic acid motif. Intermolecular recognition within **Systems I** to **III** (Scheme 1) was directed by formation of parallel hydrogen-bonded diads⁸ [**1a**·**2a**], [**1a**·**3a**] and [**1a**·**4a**]. These pre-reactive complexes may be capable of significant acceleration of the rate of formation of the corresponding triazoline cycloadducts **5a**, **6a** and **7a** (Scheme 1). Through employing this range of dipolarophiles with a varying number of methylene units in the spacer between the carboxylic acid and maleimide groups, it was intended to investigate the

entropic consequences of adding rotors to the system to rationalise any subsequent effect on the efficiency of the bimolecular complex. Here, we report: (i) dramatic acceleration observed for the reaction between azide dipole **1a** and maleimide dipolarophile **2a**, mediated by the formation of a [**1a**·**2a**] complex and (ii) the effects of the additional rotors on the kinetic behavior of these systems.

Results and discussion

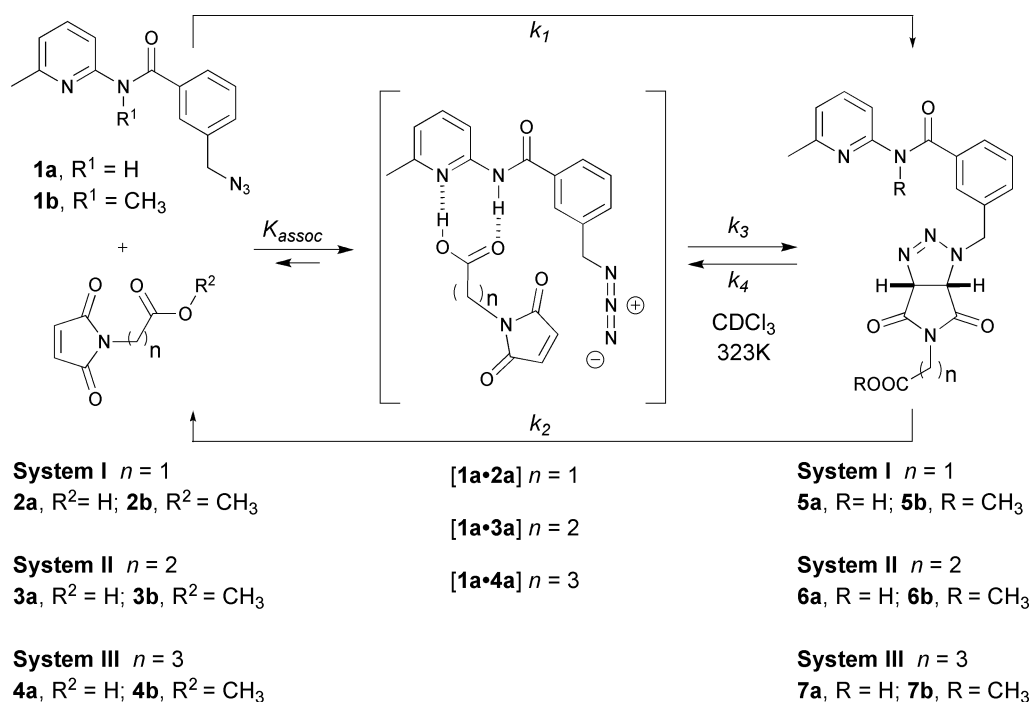
Azide **1a** was synthesized readily in two steps from commercially available 2-amino-6-picoline in 90% overall yield using standard synthetic methods. The dipolarophiles **2a** through **4a** were prepared⁹ from the corresponding amino acids in modest or moderate yield.

In order to assess the magnitude of any rate acceleration arising from the formation of a reactive binary complex, the rate of the recognition-mediated reaction must be compared to the rate of the corresponding bimolecular reaction between the two reaction partners in the absence of molecular recognition. Accordingly, the control compounds **1b**, **2b**, **3b** and **4b** were designed. These molecules do not possess the capability of **1a**, **2a**, **3a** and **4a** for molecular recognition, but match their chemical reactivity as closely as possible. The dipolarophiles were synthesised successfully from the corresponding acids **2a**, **3a** and **4a** respectively and the control dipole **1b** was synthesised in a manner analogous to that used to access dipole **1a**.

The reaction mixtures for study were prepared in CDCl₃ and the extent of reaction at 323 K assayed at regular intervals by 400 MHz ¹H NMR spectroscopy. Reaction progress was assessed by monitoring the disappearance or appearance of the appropriate resonances in the region δ 6.80 to 6.99 (maleimide) or δ 5.30 to 5.80 (cycloadducts) as a function of time. Product concentrations were calculated from the ¹H NMR spectroscopic data by deconvolution methods. All kinetic experiments were performed under thermostatically controlled conditions (± 0.1 °C). We did not observe decomposition of the triazoline products or the formation of unexpected side products in any of the kinetic experiments performed.

Centre for Biomolecular Sciences, School of Chemistry, University of St Andrews, North Haugh, St Andrews, United Kingdom KY16 9ST. E-mail: d.philp@st-andrews.ac.uk; Fax: +44 (0) 1334 463808; Tel: +44 (0) 1334 467264

† Electronic supplementary information (ESI) available: Synthetic procedures; determination of association constants; thermodynamic relationships. See DOI: 10.1039/b908072d



Scheme 1

Kinetic results for Systems I to III

In **System I**, the dipolarophile presents a single methylene rotor between the recognition site and the maleimide reactive site. The control reaction between **1b** and **2b** reveals (Fig. 1a) that, after 16 h at 323 K in CDCl₃, where [1b] = [2b] = 25.0 mM, the conversion to triazoline **5b** was 16%. Kinetic simulation and fitting of this data to the appropriate bimolecular model (k_1 and k_2 , Scheme 1) afforded the rate constant for the formation of triazoline **5b**, $k_1 = 1.62 \times 10^{-4} \text{ M}^{-1} \text{ s}^{-1}$. When the control dipole **1b** and dipolarophile **2b** were replaced by the recognition-capable dipole **1a** and dipolarophile **2a**, the rate of formation of triazoline **5a** increased dramatically. After 2 h, the conversion to triazoline **5a** was now more than 90%. In fact, the reaction reaches >90% conversion after 6 hours. At this point, the control reaction between **1b** and **2b** has reached only 8% conversion. The kinetic data obtained for the reaction between the compounds **1b** and **2b** were used to estimate the bimolecular rate constants, k_1 and k_2 , for the reaction between azide **1a** and dipolarophile **2a** according to the model outlined in Scheme 1. These estimates, together with the association constant within the

[**1a·2a**] complex (110 M⁻¹ in CDCl₃ at 323K as determined¹⁰ by ¹H NMR titration experiments) were used to perform simulations of the kinetic behaviour of the recognition-mediated system. Best-fit values for the rate constants k_3 and k_4 (Table 1) are in acceptable agreement with the experimental data and the calculated time course based on these parameters is plotted in Fig. 1a. From these parameters, the kinetic effective molarity (kEM) generated in the [**1a·2a**] complex—the ratio k_3/k_1 —was calculated as 3.96 M, indicating that the presence of the recognition elements on the reactive partners is capable of lowering the energy of the transition state for the [3+2] dipolar cycloaddition significantly. This stabilisation results in an increase of the initial rate¹¹ for the reaction between the azide and the maleimide of 125-fold ($8.1 \times 10^{-8} \text{ Ms}^{-1}$ in the control to $1.03 \times 10^{-5} \text{ Ms}^{-1}$ in the recognition mediated reaction).

The introduction of an additional methylene unit into the dipolarophile component of the [3+2] dipolar cycloaddition reaction affords **System II** (Scheme 1). The recognition-mediated reaction between **1a** and **3a** would be expected to be significantly slower than that observed for **System I** as a result of the presence

Table 1 Best-fit kinetic parameters for the three recognition-mediated dipolar cycloaddition reactions studied

System	Dipolarophile	$K_{\text{assoc}}/\text{M}^{-1a}$	$k_1/10^{-6} \text{ M}^{-1} \text{ s}^{-1}$	$k_2/10^{-6} \text{ s}^{-1b}$	$k_3/10^{-6} \text{ s}^{-1c}$	$k_4/10^{-6} \text{ s}^{-1c}$	kEM/mM ^d	tEM/mM ^e
I	2a	110	162 ± 0.0001	5.69 ± 0.02	642 ± 0.01	7.23 ± 0.04	3960	3120
II	3a	45	85.6 ± 0.001	0.77 ± 0.15	43.6 ± 0.01	7.53 ± 0.14	509	520
III	4a	45	74.2 ± 0.001	0.012 ^f	22.5 ± 0.01	1.27 ± 0.14	303	0.51 ^f

^a In CDCl₃, at 323K. ^b Best fit values derived from kinetic data acquired from the control reaction between azide **1b** and the appropriate control dipolarophile (**2b**, **3b** or **4b**). A simple reversible bimolecular reaction model was used to fit the experimental kinetic data. ^c Best fit values derived from kinetic data acquired from the recognition-mediated reaction between azide **1a** and the indicated dipolarophile. The kinetic model depicted in Scheme 1 was used to fit the experimental kinetic data. ^d kEM = k_3/k_1 . ^e tEM = k_1k_4/k_2k_3 . ^f Because of their small magnitude, these values are associated with significant uncertainty.

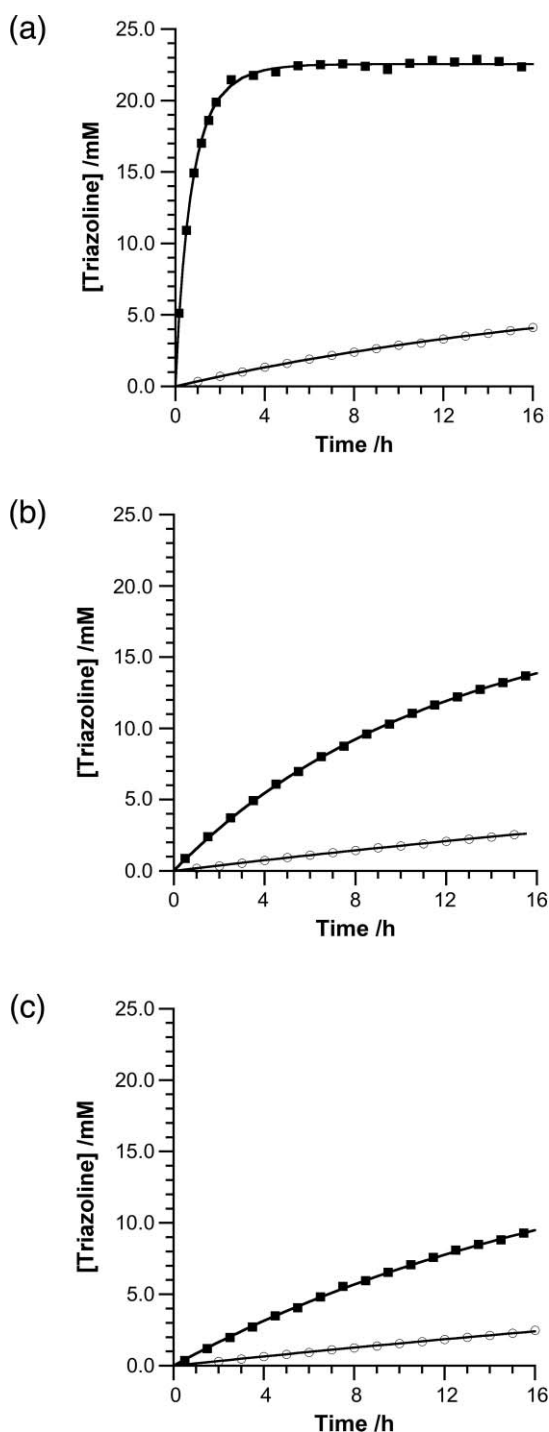


Fig. 1 Rate profiles at 50 °C for the formation of (a) triazolines **5a** (■) or **5b** (○), (b) triazolines **6a** (■) or **6b** (○) and (c) triazolines **7a** (■) or **7b** (○). In all cases, the starting concentrations of dipole and dipolarophile were 25 mM in CDCl₃ solution. In all cases, the solid lines represent the best fit of the experimental data to the appropriate kinetic model (Scheme 1) obtained using the COPASI package.²¹ See ESI† for further details of the kinetic models used.

of the extra methylene rotor in the dipolarophile **3a**. The presence of this extra rotor would be expected to have an adverse effect on the entropy of activation as it must be frozen in order to reach the transition state. The magnitude¹² of this effect should be between

13 and 21 eu. Once again, the control reaction between azide **1b** and dipolarophile **3b** at 323 K where $[1b] = [3b] = 25.0$ mM was slow—conversion to triazolines **6b** reaching 10% after 16 h (Fig. 1b). Incorporating molecular recognition into this system (**1a** and **3a**) does result in a faster reaction, however the acceleration is more modest than that observed in **System I**. The reaction rates extracted from the bimolecular reaction between **1b** and **3b** and the association constant within the complex $[1a \cdot 3a]$ (45 M^{-1} in CDCl₃ at 323 K as determined by ¹H NMR spectroscopy) were applied, as for **System I**, to the kinetic model shown in Scheme 1 and best fit values of k_3 and k_4 were determined. From these kinetic parameters (Table 1), a kEM¹³ value of 0.52 M was calculated for **System II**.

Placing a CH₂CH₂CH₂ spacer between the carboxylic acid and the maleimide unit of the dipolarophile generates **System III** (Scheme 1). Once again, we studied the kinetics of the reaction between azide **1a** and maleimide **4a** in CDCl₃ at an initial concentration of 25 mM for each component and a temperature of 323 K. The corresponding control reaction between **1b** and **4b**, performed under identical conditions, was used to establish the background rate for the recognition-mediated system. Again, both reactions were monitored by ¹H NMR spectroscopy as described previously. Deconvolution of the appropriate resonances in the time course spectra obtained allowed rate profiles for the two reactions to be constructed (Fig. 1c). As before, the reaction rates extracted from the bimolecular reaction between **1b** and **4b** and the association constant within the complex $[1a \cdot 4a]$ (45 M^{-1} in CDCl₃ at 323 K) were applied, to the kinetic model shown in Scheme 1 and best fit values of k_3 and k_4 were determined. From these kinetic parameters (Table 1), a kEM value of 0.32 M was calculated for **System III**. This value is rather close to that obtained for **System II** which possesses one less methylene rotor.

The kinetic data shown in Table 1 can be converted into free energy profiles (Fig. 2) by application of standard thermodynamic relationships. These profiles show the relative energies of the ground states and the transition state energies of the recognition-mediated reaction between azide **1a** and maleimide **2a** (Fig. 2a), as well as the relative energies for the reactions between **1a** and **3a** (Fig. 2b) and **1a** and **4a** (Fig. 2c).

The ground state of product **5a** is stabilized significantly (Fig. 2a) suggesting that the recognition that is used to assemble the $[1a \cdot 2a]$ complex lives on in the product **5a**. For the other two systems studied (Fig. 2b and c), the transition state stabilization within the binary complex is not sufficient to offset the free energy change associated with forming the complex in the first place. Thus, for both of these cases, the kinetic effective molarity is <1 M. We were, however, intrigued by the similarity in the kEM values obtained for **Systems II** and **III**. The addition of additional methylene groups into the spacer between the carboxylic acid recognition site and the maleimide should affect the rate of the cycloaddition between the azide and the dipolarophile in a predictable manner. The incorporation of additional rotors should introduce¹² an entropic penalty of between 13 and 21 eu. This entropic penalty can be converted readily to differences in rate by standard transformations allowing us to calculate the expected rates (Fig. 3) of the reaction between **1a** and the dipolarophiles **2a**, **3a** and **4a**. We performed¹⁴ this calculation in two ways. We assumed that the rate of **System I** is representative and then applied the entropic correction for the addition of one or two rotors

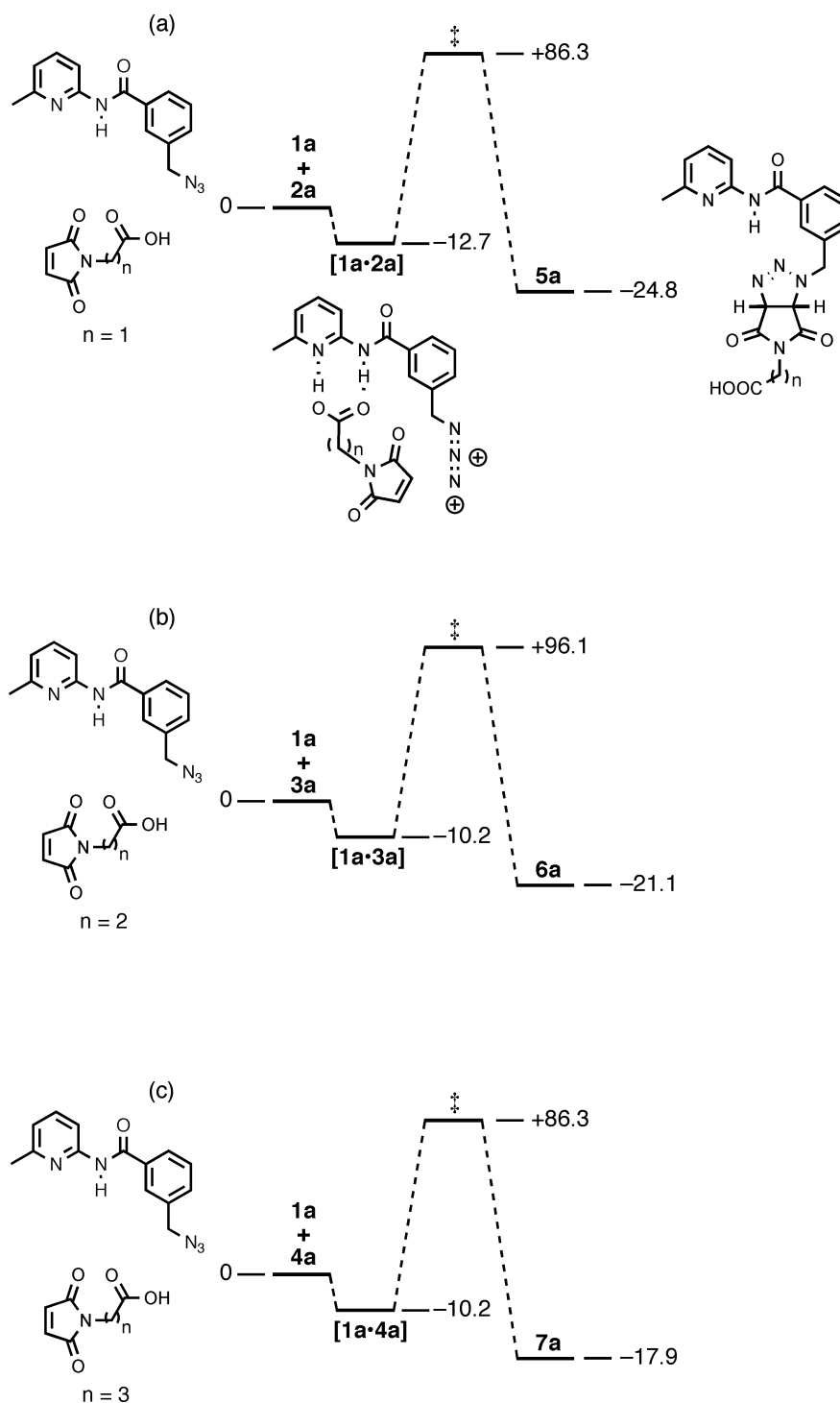


Fig. 2 Energy profiles for the formation of (a) triazoline **5a**, (b) triazoline **6a** and (c) triazoline **7a**. All energies are relative to the starting materials and are in kJ mol^{-1} .

(Fig. 3a). Alternatively, we assumed that the rate of **System III** is representative and then applied the entropic correction for the removal of one or two rotors (Fig. 3b). The dashed lines in Fig. 3 represent the boundaries for the range (13 to 21 eu) of the entropic rotor increment. From the data presented in Fig. 3, it is clear that **System II** appears to be unusually unreactive no matter which system (**I** or **III**) we take as our baseline.

In order to probe the reasons behind these reactivity differences in systems which are apparently very similar in a structural sense, we turned to computational methods. Firstly, we decided to probe the low energy conformations occupied by cycloadducts **5a**, **6a** and **7a**. We reasoned that, since the transition state for the azide cycloaddition is relatively late, we could use this conformational mapping to detect interactions which might stabilize or destabilize

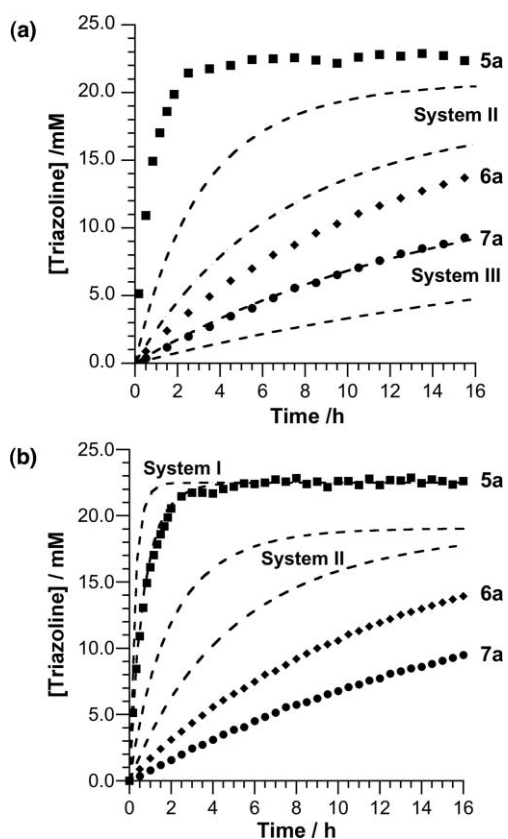


Fig. 3 Comparison of experimental rate profiles as 50 °C for the formation of triazoline **5a** (■), **6a** (◆) and **7a** (●) and computed rate profiles based on rotor increments. In both cases, the dashed lines represent the predicted course of the reaction between azide **1a** and the appropriate maleimide at 50 °C using a rotor increment of $\Delta S_{\ddagger}^{\ddagger} = +13 \text{ J mol}^{-1} \text{ K}^{-1}$ (upper line) or $\Delta S_{\ddagger}^{\ddagger} = +21 \text{ J mol}^{-1} \text{ K}^{-1}$ (lower line). Plot (a) uses **System I** as the basis for the extrapolation to **System II** and **System III** (addition of rotors) whereas plot (b) uses **System III** as the basis for the extrapolation to **System II** and **System I** (removal of rotors).

the corresponding transition states. Conformational searches were carried out using Monte Carlo methods and conformations within 50 kJ mol⁻¹ of the global minimum were saved. The results of these searches are shown in Fig. 4. In Fig. 4, the low energy conformations of the cycloadducts are plotted as a function of two hydrogen bonding distances—the N–H(Amide)···O=C(Acid) distance and the N(Pyridine)···H–O(Acid) distance. The shading of the individual points represents the relative energy of the conformations—the darker the shading, the lower the energy.

This conformational mapping reveals three distinct families of low energy conformations. Representative structures from each family for cycloadduct **6a** (**System II**) are shown in Fig. 5—the families for both **5a** and **7a** are very similar (see ESI†). **Family B** structures are characterized by a hydrogen bond between the carboxylic acid proton and the carbonyl group of the amidopyridine. **Family C** structures are characterized by a hydrogen bond between the carboxylic acid carbonyl oxygen atom and the N–H group of the amidopyridine. It seemed unlikely that either of these conformations had any direct bearing on the reactivity of the maleimide. However, the structures in **Family A** contain a N(Pyridine)···H–O(Acid) hydrogen bond and some of them also contain a hydrogen bond between the amide N–H and the

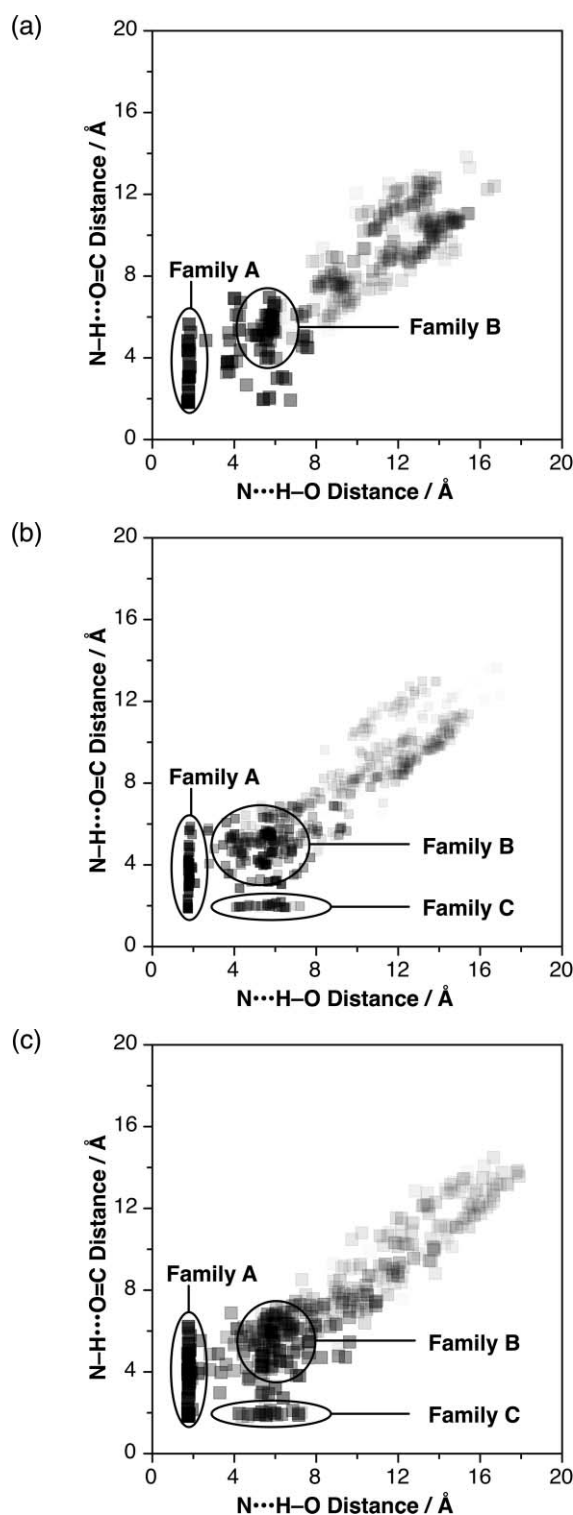


Fig. 4 Comparison of low energy conformations adopted by triazolines (a) **5a**, (b) **6a** and (c) **7a** calculated using the OPLS_2005 forcefield and the GB/SA solvation model for chloroform. In each case, individual conformations are represented by a square which is shaded according to its energy relative to the global minimum with black being the global minimum and white being + 50 kJ mol⁻¹. Conformations are set out as a function of two hydrogen bonding distances—the pyridine N to acid proton distance (*x* axis) and the amide proton to acid carbonyl oxygen atom distance (*y* axis).

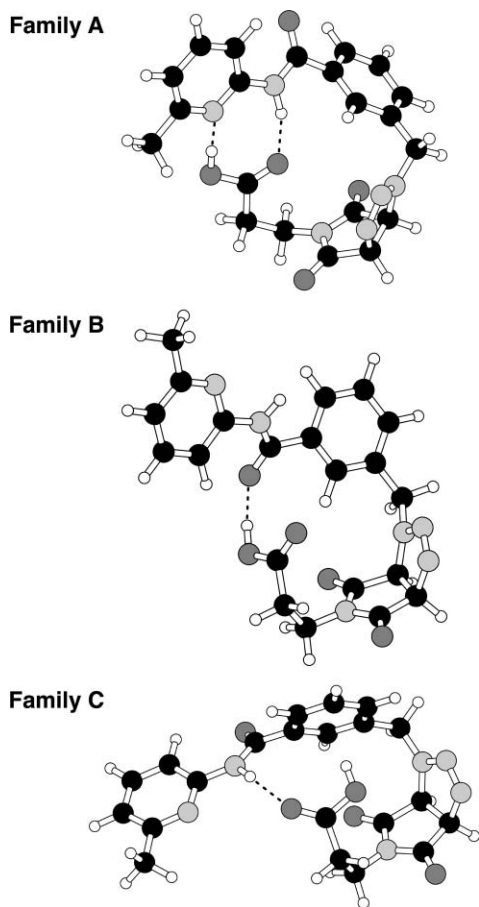


Fig. 5 Ball and stick representations of examples of conformations from each of the three families identified in Fig. 4. Conformations are shown for **6a** only—those adopted by **5a** and **7a** have the same structural features. The type of conformation shown for **Family A** is described as normally hydrogen bonded in the text. Carbon atoms are shaded black, oxygen atoms are shaded dark grey, nitrogen atoms are shaded light grey and hydrogen atoms are unshaded. Dashed lines represent hydrogen bonds.

carbonyl oxygen of the acid—the global minimum is one such structure. This conformation is the one that we had anticipated would play a major role in the acceleration of the reaction in our original design.

Surprisingly, there are, however, a number of low energy structures which, although they have a hydrogen bond between the pyridine N atom and the acid hydrogen do not contain a N–H(Amide)⋯O=C(Acid) hydrogen bond. In the case of **5a**, the lowest energy of these conformations (Fig. 6a), although very close in energy to the global minimum (+8.04 kJ), does not contain any additional interactions. However, in the case of **6a** and **7a**, in the lowest energy of these conformations (+7.41 kJ and +5.69 kJ, respectively) (Fig. 6b and c) there is an additional hydrogen bond present between the N–H of the amide group and one of C=O groups on the maleimide. Clearly, the short tether length present in **5a** prevents this type of conformation being stable since the lowest energy conformation which possesses such an additional interaction is +30.79 kJ higher in energy than the global minimum. The presence of this hydrogen bond in these conformations in **6a** and **7a** opens up the possibility that the reactivity of the maleimide

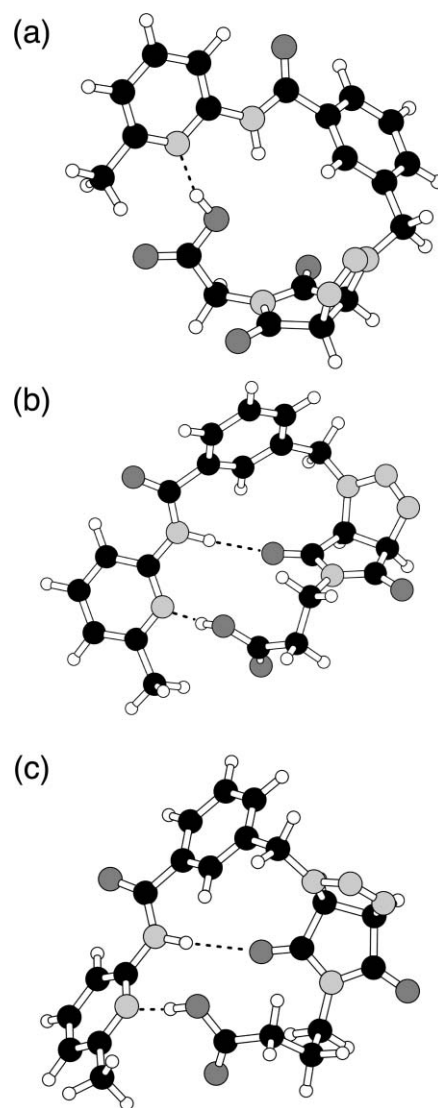


Fig. 6 Ball and stick representations of examples of conformations from **Family A** for (a) **5a**, (b) **6a** and (c) **7a** which do not display a hydrogen bond between the amide proton and acid carbonyl oxygen atom. The type of conformations shown in (b) and (c) are described as abnormally hydrogen bonded in the text. Carbon atoms are shaded black, oxygen atoms are shaded dark grey, nitrogen atoms are shaded light grey and hydrogen atoms are unshaded. Dashed lines represent hydrogen bonds.

may be altered¹⁵ by hydrogen bond-mediated polarization in the transition states leading to these products.

In order to probe the effect of this interaction further, we turned to electronic structure calculations. We located transition state structures linking the binary complexes [**1a**·**2a**], [**1a**·**3a**] and [**1a**·**4a**], in both the normal and abnormally hydrogen bonded forms, and the corresponding cycloadducts at the B3LYP/6-31G(d,p) level of theory. Additionally, we calculated the transition state linking benzyl azide and *N*-methylmaleimide and the corresponding cycloadduct in order to allow comparison with a situation where recognition is not involved. The results of these calculations provide some insight into the subtle structural effects which operate in these systems and help to rationalise the reasons for the relatively poor performance of **System II**. The structures of

the five transition states located—two each for **Systems I** and **III** and one for **System II**—are shown in Fig. 7.

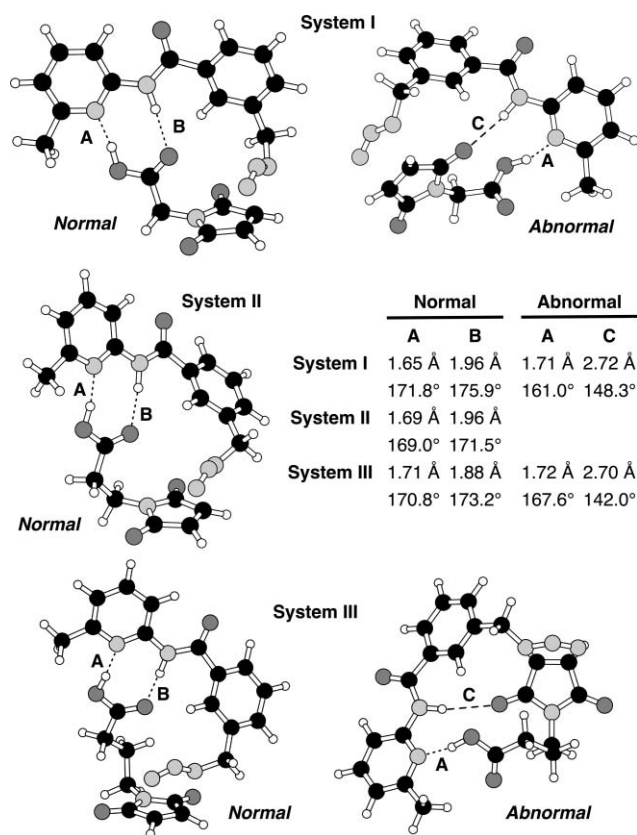


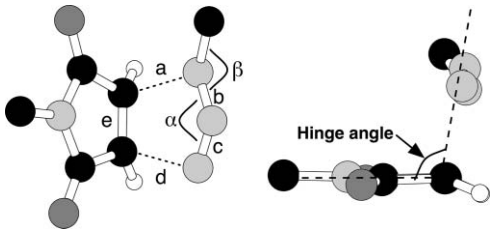
Fig. 7 Ball and stick representations of the transition states accessible to the complexes (a) [1-2a], (b) [1-3a] and (c) [1-4a]. Carbon atoms are shaded black, oxygen atoms are shaded dark grey, nitrogen atoms are shaded light grey and hydrogen atoms are unshaded. Dashed lines represent hydrogen bonds.

We can immediately rule out any role for a hydrogen bond between the N–H of the amide group and one of the C=O groups on the maleimide in altering the reactivity of the maleimide dipolarophile. In all cases, the N–H...O=C distance is greater than 2.50 Å. We have shown previously^{15a} that even two short N–H...O=C hydrogen bonds to a maleimide have a limited effect on the reactivity of the system in dipolar cycloaddition reactions. Given the long N–H...O=C distances present here, we would expect that these contacts play essentially no role. In all cases where transition states were located successfully, there are minimal structural differences (Table 2) between the transition state structure in the hydrogen bonded complex and that for the bimolecular reaction between benzyl azide and *N*-methylmaleimide. In the case of **System I**, the lowest energy transition state—by some 27.6 kJ mol⁻¹—is that accessed from the normally hydrogen bonded complex. This transition state is the one accessed from the global minimum conformation. In the case of **System III**, the lowest energy transition state—by 5.1 kJ mol⁻¹—is, once again, that accessed from the normally hydrogen bonded complex, *i.e.* the one accessed from the global minimum conformation. Therefore, in these two cases, two reaction pathways are accessible—one through the normally hydrogen bonded complex and one through the abnormally hydrogen bonded complex. By contrast, in the case

of **System II**, only the transition state from the normally hydrogen bonded complex is accessible. Repeated attempts to locate the transition state that would be accessed from the abnormally hydrogen bonded complex in **System II** resulted in the location of the transition state accessed by the normally hydrogen bonded complex instead.

The accessibility of transition states with different structural types for each complex makes direct comparison of the relative rates of reaction through these complexes problematic¹⁶ using electronic structure methods. Bruice and Lightstone have demonstrated¹⁶ that there is a correlation between rate and the fraction of low energy near attack conformations (NACs)—the higher the mole fraction of NACs the faster the reaction. This analysis is particularly suited to our system as the definition of a NAC relies only on the relative orientations of the reacting centres and not on the location of the recognition elements. Accordingly, we adapted the protocol described by Bruice and Lightstone to our systems. Stochastic methods were used¹⁷ to generate >25000 conformations for each of the complexes, [1-2a], [1-3a] and [1-4a]. The generation of these conformations was subject to a single constraint—the hydrogen bond between the amidopyridine nitrogen atom and the carboxylic acid proton must be maintained. After removal of conformations that were not local minima, those that were >25 kJ mol⁻¹ from the global minimum and duplicate conformations, a set of low energy conformations for each complex was created. These sets consisted of 198 conformations for [1-2a], 176 conformations for [1-3a] and 220 conformations for [1-4a]. These sets were then searched for conformations which satisfied our definition¹⁸ of a NAC for the dipolar cycloaddition reaction. This analysis revealed that of the 198 conformations for [1-2a], 22 were NACs, of the 176 conformations for [1-3a], 11 were NACs and of the 220 conformations for [1-4a], 25 were NACs. The locations of the NACs within the energy distribution of the lowest conformations for each complex are shown in Fig. 8a. Since, in each case, the NACs are of varying energy with respect to the global minimum, it is necessary to account for the probability of a NAC being occupied at 313 K. Thus, for each complex, the overall Boltzmann-weighted probability of the occurrence of a NAC was 0.082 for [1-2a], 0.028 for [1-3a], and 0.026 for [1-4a].

There is a reasonable correlation (Fig. 8b) between the computed initial rate of reaction based on the experimentally determined rate constants and the Boltzmann-weighted probability of the occurrence of a NAC. Thus, for **System I**, we would expect that the high fraction of low energy NACs, coupled with the higher association constant for the [1-2a] complex, would result in rapid reaction through this complex. In the case of **System III**, the additional flexibility of the three carbon atom spacer connecting the maleimide to the acid recognition site lowers the fraction of NACs; however, a substantial fraction of the accessible low energy conformations are NACs. The anomalous member of this series would therefore appear to be **System II** and can be traced to the relatively low fraction of low energy conformations that are NACs. The net result is that **System II** displays reactivity which is much closer to **System III** than to **System I**. Phenomenologically, these findings mirror the results reported¹⁹ by Hamilton and co-workers—the inclusion of added free rotors in their thiol transacylase mimic removes the advantage of the close proximity of the reactive groups to each other.

Table 2 Calculated structural parameters for the transition states accessed by **Systems I, II and III**


Metric ^a	System I		System II	System III		Base TS ^c
	Normal ^b	Abnormal ^b	Normal ^b	Normal ^b	Abnormal ^b	
Relative Energy/kJ mol ⁻¹	0	+ 27.6	–	0	+ 5.10	–
a/Å	2.068	2.072	2.090	2.086	2.113	2.095
b/Å	1.263	1.262	1.261	1.265	1.269	1.266
c/Å	1.174	1.175	1.173	1.174	1.175	1.174
d/Å	2.178	2.221	2.218	2.195	2.147	2.188
e/Å	1.394	1.389	1.380	1.389	1.392	1.391
α/°	138.0	137.5	139.6	138.3	138.2	138.2
β/°	120.6	123.8	122.9	121.7	117.7	120.6
Hinge angle/°	102.4	101.8	100.6	102.5	101.3	102.3
Bond Order C–N ^a	0.347	0.333	0.329	0.336	0.340	0.331
Bond Order C–N ^a	0.348	0.332	0.325	0.344	0.361	0.341

^a From calculation at B3LYP/6-31G(d,p) level of theory. ^b Normal and Abnormal refer to hydrogen bonding pattern adopted in the transition state. See Fig. 7 and text for details. ^c From reaction of benzyl azide with *N*-methylmaleimide.

Conclusions

The design of supramolecular systems which can achieve the acceleration and control of chemical reactions remains a challenging goal. We have demonstrated that, with a correctly designed system, such as **System I**, it is possible to accelerate a cycloaddition reaction by two orders of magnitude. This level of rate acceleration is competitive²⁰ with catalytic antibodies which catalyze similar reactions. However, the subtle interplay between structure and reactivity is hard to predict even in systems in which the structural variation is as simple as the examples described here. Therefore, we expect that significant progress towards the goal of simple recognition-based approaches to the acceleration and control of chemical reactions will require the continued and expanded application of diverse computational methods as well as synthetic chemistry to the design of recognition-mediated reactive supramolecular assemblies.

Experimental section

General procedures

Chemicals and solvents were purchased from standard commercial suppliers and were used as received unless otherwise stated. Tetrahydrofuran (THF) was dried by heating to reflux in the presence of sodium/benzophenone under an N₂ atmosphere and was collected by distillation. Acetonitrile (CH₃CN), dichloromethane (DCM) and chloroform were dried by heating under reflux over calcium hydride and distilled under N₂. Acetone and triethylamine were distilled over K₂CO₃.

Thin-layer chromatography (TLC) was performed on aluminium plates coated with Merck Kieselgel 60 F₂₅₄. Developed plates were air-dried and scrutinised under a UV lamp (366 nm),

and where necessary, stained with iodine, phosphomolybdic acid (PMA), ninhydrin or potassium permanganate to aid visualisation. Column chromatography was performed using Kieselgel 60 (0.040–0.063 mm mesh, Merck 9385) or MP Silica (silica gel, 0.032–0.063 mesh). Melting points were determined using an Electrothermal 9200 melting point apparatus and are reported uncorrected. Microanalyses (C, H, N) were carried out at the University of St Andrews. Infra-red Spectra (IR) were recorded as KBr discs or thin films (PTFE plates) using a Perkin-Elmer Paragon 1000 spectrometer. ¹H Nuclear Magnetic Resonance (NMR) spectra were recorded on a Bruker Avance 400 (400.1 MHz), a Varian Gemini 2000 (300.0 MHz), or a Varian UNITYplus 500 (500.1 MHz) spectrometer using deuterated solvent as the lock and the residual solvent as the internal reference in all cases. ¹³C NMR spectra using the PENDANT sequence were recorded on a Bruker Avance 300 (75.5 MHz) spectrometer. All other ¹³C spectra were recorded on a Varian Gemini 2000 (75.5 MHz) spectrometer using composite pulse ¹H decoupling. All spectra were recorded at 298 K unless otherwise stated. All coupling constants (*J*) are quoted to the nearest 0.1 Hz. In the assignment of ¹H NMR spectra the symbols br, s, d, t, q and m denote broad, singlet, doublet, triplet, quartet and multiplet, respectively.

Electron impact mass spectrometry (EIMS) and high-resolution mass spectrometry (HRMS) were carried out on a VG AUTOSPEC mass spectrometer on a Micromass GCT orthogonal acceleration time of flight mass spectrometer. Chemical Ionisation Mass Spectrometry (CIMS) was carried out on a VG AUTOSPEC instrument or on a Micromass GCT orthogonal acceleration time of flight mass spectrometer. Electrospray mass spectrometry (ESMS) and high-resolution mass spectrometry (HRMS) was carried out on a Micromass LCT orthogonal time of flight mass spectrometer.

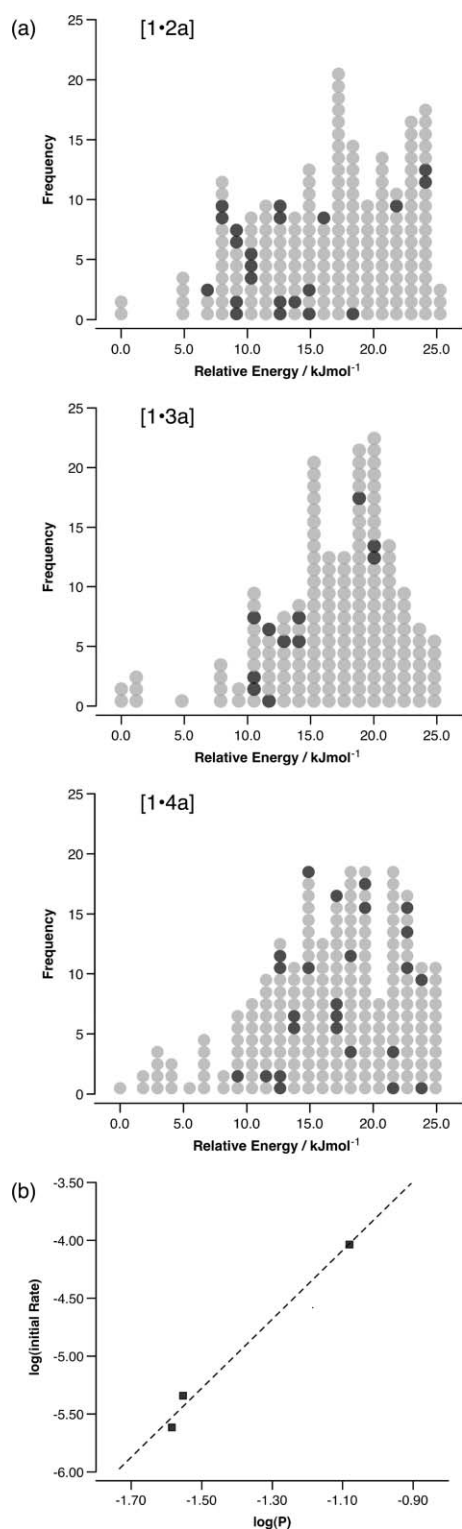


Fig. 8 (a) Distribution of Near Attack Conformations (NACs) within the sets of low energy conformations identified for (i) [1·2a], (ii) [1·3a] and (iii) [1·4a]. Each circle represents a low energy conformation, NACs are coloured black and non-NACs are coloured grey. (b) Correlation between initial rate and the Boltzmann-weighted probability of the occurrence of a NAC. The initial rate values are calculated from the rate constants and equilibrium constants shown in Table 1, assume a starting concentration of 25 mM and include contributions from both the bimolecular and recognition-mediated pathways. A regression line is provided to guide the eye.

General procedure for kinetic experiments

Stock solutions were prepared by dissolving the appropriate amount of reagent in CDCl_3 using a 2 cm^3 ($2 \text{ cm}^3 \pm 0.02 \text{ cm}^3$ accuracy) volumetric flask. Masses of reagents were measured using a Sartorius BP 211D balance ($\pm 0.01 \text{ mg}$). Stock solutions were pre-equilibrated to the appropriate temperature in a water bath for a minimum of 30 minutes. Subsequent experimental samples, suitable for kinetic experiments, were obtained by mixing a fixed amount of appropriate stock solutions by using Hamilton gas-tight syringes in a Wilmad 507PP or 528PP NMR tube, which was then fitted with a polyethylene pressure cap to minimise solvent evaporation. Reaction mixtures were monitored systematically by 400 MHz ^1H NMR spectroscopy over 17 hours. The extent of reaction for kinetic experiments was determined using the deconvolution tool available in 1D WINNMR (Version 6.2.0.0, Bruker Daltonik GmbH, Germany, 2000). Kinetic simulation and fitting of the resultant data to the appropriate kinetic models was achieved using the parameter optimization mode of COPASI.²¹

Computational methods

All molecular mechanics calculations were performed on a Linux workstation and the OPLS_2005 forcefield together with the GB/SA solvation model for chloroform as implemented in MacroModel (Version 9.5, Schrödinger Inc., 2008). Electronic structure calculations were carried out using GAMESS²² running on a Linux cluster. The 64-bit Linux version dated 24 Mar 2007 (Revision 6) was used in all calculations. The transition state for the reaction between azide and maleimide was located by generation of an initial guess using the linear synchronous transit (LST) method and then refinement at the HF/6-31G(d) level of theory within GAMESS. This model transition state was then used to construct an initial guess for the transition state leading to the appropriate cycloadduct. This guess was refined at the B3LYP/6-31G(d,p) level of theory to a transition state structure possessing single imaginary vibration that corresponded to the reaction coordinate. Relative energies are computed using standard methods from the electronic energies and the results of the vibrational analysis performed on the structures.

Synthetic procedures

Preparative methods and characterisation data for compounds **1a**, **1b**, **2a**, **2b**, **3a**, **3b**, **4a**, **4b**, **8**, **9** are provided in the ESI.†

1-(*N*-{6-Methyl-2-pyridyl}-benzamid-3-yl)methyl-4,6-dioxo-3a,4,6a-tetrahydro-1*H*-pyrrolo [3,4-*d*][1,2,3]triazol-5-yl)-2-ethanoic acid (5a**). A solution of 2-maleimidoethanoic acid (**2a**, 78 mg, 0.5 mmol) and azide **1a** (134 mg, 0.5 mmol) in dry chloroform (5 mL) was heated at 50 °C for 24 hours. The resultant precipitate was removed by filtration and washed thoroughly with hexane before it was dried under high vacuum to afford the desired triazoline **5a** (163 mg, 77%) as a white solid. Mp = 249–251.5 °C; ν_{max} (KBr) (cm^{-1}) = 3470, 3063, 3002, 1703, 1583; ^1H NMR (300 MHz, CDCl_3) δ = 12.12 (1H, bs, NH), 8.41 (1H, d, $^3J_{\text{HH}}$ = 8.5 Hz, ArCH), 8.02–8.00 (2H, m, ArCH), 7.89 (1H, dd, $^3J_{\text{HH}}$ = 7.5 Hz, $^3J_{\text{HH}}$ = 7.5 Hz, ArCH), 7.51–7.48 (2H, m, ArCH), 7.04 (1H, d, $^3J_{\text{HH}}$ = 7.5 Hz, ArCH), 5.80 (1H, d, $^3J_{\text{HH}}$ = 10.5 Hz, CH), 5.42 (1H, d, $^3J_{\text{HH}}$ = 15.5 Hz, CHH), 4.73 (1H, d,**

$^3J_{\text{HH}} = 15.5$ Hz, *CHH*), 4.46 (1H, d, $^3J_{\text{HH}} = 17.0$ Hz, *CHH*), 4.38 (1H, d, $^3J_{\text{HH}} = 10.5$ Hz, *CH*), 4.12 (1H, d, $^3J_{\text{HH}} = 17.0$ Hz, *CHH*), 2.55 (3H, s, *CH*₃); ¹³C NMR (75 MHz, d₆-DMSO) $\delta = 172.1$ (C), 170.8 (C), 168.0 (C), 165.8 (C), 156.8 (C), 151.7 (C), 138.7 (ArCH), 135.9 (C), 134.7 (C), 132.0 (ArCH), 129.0 (ArCH), 128.2 (ArCH), 127.8 (ArCH), 119.4 (ArCH), 111.9 (ArCH), 82.2 (CH), 57.8 (CH), 52.1 (CH₂), 40.5 (CH₂), 23.7 (CH₃); LRMS (ES): *m/z* (%) = 423 (100) [M + H]⁺; HRMS: found 445.1234 [M + Na]⁺, C₂₀H₁₈N₆O₅Na requires 445.1236.

1-([N-{6-Methyl-2-pyridyl}-benzamid-3-yl]methyl-4,6-dioxo-3a,4,6a-tetrahydro-1H-pyrrolo [3,4-d][1,2,3]triazol-5-yl)-3-propanoic acid (6a). A solution of 3-maleimidopropanoic acid (**3a**, 68 mg, 0.4 mmol) and azide **1a** (107 mg, 0.4 mmol) in dry chloroform (4 mL) was heated at 50 °C for 24 hours. The precipitate formed was filtered off and was washed with hexane. The residue so obtained was dried under high vacuum to give the cycloadduct **6a** (127 mg, 73%) as a white solid. Mp = 260–262 °C; Elemental analysis calcd. (%) for C₂₁H₂₀N₆O₅: C, 57.79; H, 4.62; N, 19.26; Found: C, 57.78; H, 4.60; N, 19.42; ν_{max} (KBr) (cm⁻¹) = 3483, 3210, 2992, 1711, 1682, 1556; ¹H NMR (300 MHz, d₆-DMSO) $\delta = 10.75$ (1H, bs, *NH*), 8.03–7.98 (3H, m, *ArCH*), 7.72–7.70 (1H, m, *ArCH*), 7.53–7.51 (2H, m, *ArCH*), 7.04 (1H, d, $^3J_{\text{HH}} = 7.5$ Hz, *ArCH*), 5.61 (1H, d, $^3J_{\text{HH}} = 11.0$ Hz, *CH*), 5.24 (1H, d, $^3J_{\text{HH}} = 15.5$ Hz, *CHH*), 4.87 (1H, d, $^3J_{\text{HH}} = 15.5$ Hz, *CHH*), 4.35 (1H, d, $^3J_{\text{HH}} = 11.0$ Hz, *CH*), 3.58 (2H, t, $^3J_{\text{HH}} = 7.5$ Hz, *CH*₂), 2.51 (2H, t, $^3J_{\text{HH}} = 7.5$ Hz, *CH*₂), 2.45 (3H, s, *CH*₃); ¹³C NMR (75 MHz, d₆-DMSO) $\delta = 172.1$ (C), 171.7 (C), 170.9 (C), 165.5 (C), 156.5 (C), 151.4 (C), 138.3 (ArCH), 135.7 (C), 134.4 (C), 131.6 (ArCH), 128.6 (ArCH), 127.9 (ArCH), 127.4 (ArCH), 119.0 (ArCH), 111.6 (ArCH), 81.9 (CH), 57.5 (CH), 51.7 (CH₂), 34.4 (CH₂), 31.1 (CH₂), 23.5 (CH₃); LRMS (ES): *m/z* (%) = 437 (100) [M + H]⁺, 409 (15); HRMS: found 459.1385 [M + Na]⁺, C₂₁H₂₀N₆O₅Na requires 459.1393.

1-([N-{6-Methyl-2-pyridyl}-benzamid-3-yl]methyl-4,6-dioxo-3a,4,6a-tetrahydro-1H-pyrrolo [3,4-d][1,2,3]triazol-5-yl)-4-n-butanoic acid (7a). A solution of 4-maleimidobutanoic acid (**4a**, 73 mg, 0.4 mmol) and azide **1a** (107 mg, 0.4 mmol) in dry chloroform (4 mL) was heated at 50 °C for 24 hours. The resultant precipitate was removed by filtration and washed thoroughly with hexane before it was dried under high vacuum to afford the desired triazoline **6a** (129 mg, 72%) as a white powder. Mp = 280.5–282.5 °C; Elemental analysis calcd. (%) for C₂₂H₂₂N₆O₅: C, 58.66; H, 4.92; N, 18.66; Found: C, 58.45; H, 4.97; N, 18.62; ν_{max} (KBr) (cm⁻¹) = 3482, 3252, 3078, 1707, 1666, 1579; ¹H NMR (300 MHz, d₆-DMSO) $\delta = 10.77$ (1H, bs, *NH*), 8.01–7.97 (3H, m, *ArCH*), 7.69–7.65 (1H, m, *ArCH*), 7.53–7.51 (2H, m, *ArCH*), 7.03 (1H, d, $^3J_{\text{HH}} = 7.0$ Hz, *ArCH*), 5.63 (1H, d, $^3J_{\text{HH}} = 11.0$ Hz, *CH*), 5.25 (1H, d, $^3J_{\text{HH}} = 15.0$ Hz, *CHH*), 4.85 (1H, d, $^3J_{\text{HH}} = 15.0$ Hz, *CHH*), 4.32 (1H, d, $^3J_{\text{HH}} = 11.0$ Hz, *CH*), 3.45 (2H, m, *CH*₂), 2.48 (3H, s, *CH*₃), 2.18 (2H, m, *CH*₂), 1.68 (2H, m, *CH*₂); ¹³C NMR (75 MHz, d₆-DMSO) $\delta = 173.7$ (C), 172.6 (C), 171.5 (C), 165.6 (C), 156.6 (C), 151.5 (C), 138.5 (ArCH), 135.8 (C), 134.5 (C), 131.8 (ArCH), 128.7 (ArCH), 128.0 (ArCH), 127.6 (ArCH), 119.2 (ArCH), 111.7 (ArCH), 82.1 (CH), 57.7 (CH), 51.8 (CH₂), 37.8 (CH₂), 30.6 (CH₂), 23.6 (CH₃), 22.3 (CH₂); LRMS (ES): *m/z* (%) = 473 (85) [M + Na]⁺, 451 (36) [M + H]⁺, 445 (47), 423 (100); HRMS: found 473.1551 [M + Na]⁺, C₂₂H₂₂N₆O₅Na requires 473.1549.

Acknowledgements

We thank the EPSRC for financial support (Grant EP/E017851/1). We thank Prof. G von Kiedrowski for providing us with his SimFit program.

Notes and references

- For some reviews see: (a) R. Breslow, *Acc. Chem. Res.*, 1995, **28**, 146; (b) Y. Murakami, J. Kikuchi, Y. Hisaea and O. Hayashida, *Chem. Rev.*, 1996, **96**, 721; (c) A. J. Kirby, *Angew. Chem., Int. Ed. Engl.*, 1996, **35**, 707; (d) H. Dugas, *Bioorganic Chemistry - A Chemical Approach to Enzyme Action*, Third Edition; Springer-Verlag, New York, 1996; (e) M. I. Page, *Philos. Trans. R. Soc. Lond. B*, 1991, **332**, 149; (f) A. J. Kirby, *Phil. Trans. R. Soc. Lond. A*, 1993, **345**, 67; (g) F. M. Menger, *Acc. Chem. Res.*, 1993, **26**, 206; (h) D. Philp, A. Robertson and A. J. Sinclair, *Chem. Soc. Rev.*, 2000, **29**, 141.
- (a) T. S. Koblenz, J. Wassenaar and J. N. H. Reek, *Chem. Soc. Rev.*, 2008, **37**, 247; (b) Z. Yan, T. McCracken, S. Xia, V. Maslak, J. Gallucci, C. M. Hadad and J. D. Badjic, *J. Org. Chem.*, 2008, **73**, 355; (c) C. Schmuck, *Angew. Chem., Int. Ed.*, 2007, **46**, 5830; (d) M. D. Pluth, R. G. Bergman and K. N. Raymond, *Angew. Chem., Int. Ed.*, 2007, **46**, 8587; (e) D. Ajami, M. P. Schramm, A. Volontario and J. Rebek, *Angew. Chem., Int. Ed.*, 2007, **46**, 242; (f) T. Furusawa, M. Kawano and M. Fujita, *Angew. Chem., Int. Ed.*, 2007, **46**, 5717; (g) R. J. Hooley and J. Rebek, *Org. Biomol. Chem.*, 2007, **5**, 3631; (h) S. M. Butterfield and J. Rebek, *Chem. Commun.*, 2007, 1605; (i) M. Yoshizawa, M. Tamura and M. Fujita, *Science*, 2006, **312**, 251; (j) L. Zhu and E. V. Anslyn, *Angew. Chem., Int. Ed.*, 2006, **45**, 1190; (k) S. Rau, B. Schaefer, D. Gleich, E. Anders, M. Rudolph, M. Friedrich, H. Goerls, W. Henry and J. G. Vos, *Angew. Chem., Int. Ed.*, 2006, **45**, 6215; (l) D. Fiedler, H. van Halbeek, R. G. Bergman and K. N. Raymond, *J. Am. Chem. Soc.*, 2006, **128**, 10240; (m) T. Evan-Salem, I. Baruch, L. Avram, Y. Cohen, L. C. Palmer and J. Rebek, *Proc. Natl. Acad. Sci. U. S. A.*, 2006, **103**, 12296; (n) R. J. Hooley and J. Rebek, *J. Am. Chem. Soc.*, 2005, **127**, 11904; (o) M. Yoshizawa and M. Fujita, *Pure Appl. Chem.*, 2005, **77**, 1107; (p) S. Richeter and J. Rebek, *J. Am. Chem. Soc.*, 2004, **126**, 16280; (q) C. Gibson and J. Rebek, *Org. Lett.*, 2002, **4**, 1887; (r) M. Tominaga, K. Konishi and T. Aida, *J. Am. Chem. Soc.*, 1999, **121**, 7704; (s) K. Kavallieratos and R. H. Crabtree, *Chem. Commun.*, 1999, 2109; (t) J. Kang, G. Hilmersson, J. Santamaria and J. Rebek, Jr, *J. Am. Chem. Soc.*, 1998, **120**, 3650; (u) J. Kang, G. Hilmersson, J. Santamaria and J. Rebek, Jr, *J. Am. Chem. Soc.*, 1998, **120**, 7389; (v) M. Marty, Z. Clyde-Watson, L. J. Twyman, M. Nakash and J. K. M. Sanders, *Chem. Commun.*, 1998, 2265; (w) Z. Clyde-Watson, A. Vidal-Ferrán, L. J. Twyman, C. J. Walter, D. W. F. McCallien, S. Fanni, N. Bampos, R. S. Wylie and J. K. M. Sanders, *New J. Chem.*, 1998, 493; (x) C. Raposo, A. Luengo, M. Almaraz, M. Martín, M. L. Musson, M. C. Caballero and J. R. Morán, *Tetrahedron*, 1996, **52**, 12323; (y) R. Breslow and C. Schmuck, *J. Am. Chem. Soc.*, 1996, **118**, 6601; (z) P. Tecilla, V. Jubian and A. D. Hamilton, *Tetrahedron*, 1995, **51**, 435; I. Huc, J. Pieters and J. Rebek, Jr, *J. Am. Chem. Soc.*, 1994, **116**, 10296.
- (a) V. C. Allen, D. Philp and N. Spencer, *Org. Lett.*, 2001, **3**, 777; (b) J. M. Quayle, A. M. Z. Slawin and D. Philp, *Tetrahedron Lett.*, 2002, **43**, 7229; (c) E. Kassianidis, R. J. Pearson and D. Philp, *Org. Lett.*, 2005, **7**, 3833; (d) R. J. Pearson, E. Kassianidis and D. Philp, *Tetrahedron Lett.*, 2004, **45**, 4777; (e) R. J. Pearson, E. Kassianidis, A. M. Z. Slawin and D. Philp, *Chem.-Eur. J.*, 2006, **12**, 6829; (f) E. Kassianidis and D. Philp, *Angew. Chem., Int. Ed.*, 2006, **45**, 6334.
- (a) D. Philp and A. Robertson, *Chem. Commun.*, 1998, 879; (b) R. Bennes, D. Philp, N. Spencer, B. M. Kariuki and K. D. M. Harris, *Org. Lett.*, 1999, **1**, 1087; (c) A. Robertson, D. Philp and N. Spencer, *Tetrahedron*, 1999, **55**, 11365; (d) R. Bennes, M. S. Babiloni, W. Hayes and D. Philp, *Tetrahedron Lett.*, 2001, **42**, 2377; (e) E. Kassianidis, R. J. Pearson and D. Philp, *Chem.-Eur. J.*, 2006, **12**, 8798; (f) R. Bennes and D. Philp, *Org. Lett.*, 2006, **8**, 3651.
- (a) C. A. Booth and D. Philp, *Tetrahedron Lett.*, 1998, **59**, 6987; (b) H. L. Rowe, N. Spencer and D. Philp, *Tetrahedron Lett.*, 2000, **41**, 4475; (c) S. J. Howell, N. Spencer and D. Philp, *Tetrahedron*, 2001, **57**, 4945; (d) S. J. Howell, N. Spencer and D. Philp, *Org. Lett.*, 2002, **4**, 273; (e) S. M. Turega and D. Philp, *Chem. Commun.*, 2006, 3684.
- (a) M. I. Page, *Chem. Soc. Rev.*, 1973, **2**, 295; (b) A. J. Kirby, *Adv. Phys. Org. Chem.*, 1980, **17**, 183; (c) M. I. Page, *The Chemistry of Enzyme*

- Action, M. I. Page Ed., Elsevier, Amsterdam, 1984, p 1; (d) F. M. Menger, *Acc. Chem. Res.*, 1985, **18**, 128; (e) M. I. Page, *Phil. Trans. R. Soc. London B*, 1991, **332**, 149; (f) A. J. Kirby, *Philos. Trans. R. Soc. London A*, 1993, **345**, 67; (g) T. C. Bruice and F. C. Lightstone, *Acc. Chem. Res.*, 1999, **32**, 127.
- 7 (a) C. W. Tornøe, C. Christensen and M. Meldal, *J. Org. Chem.*, 2002, **67**, 3057; (b) V. V. Rostovtsev, L. G. Freen, V. V. Fokin and K. B. Sharpless, *Angew. Chem., Int. Ed.*, 2002, **41**, 2596. For a review of click chemistry; H. C. Kolb, M. G. Finn and K. B. Sharpless, *Angew. Chem., Int. Ed.*, 2001, **40**, 2004.
- 8 (a) F. García-Tellado, S. Goswami, S. K. Chang, S. Geib and A. D. Hamilton, *J. Am. Chem. Soc.*, 1990, **112**, 7395; (b) A. D. Hamilton and S. C. Hirst, *J. Am. Chem. Soc.*, 1991, **113**, 382.
- 9 R. J. Pearson, E. Kassianidis, A. M. Z. Slawin and D. Philp, *Org. Biomol. Chem.*, 2004, **2**, 3434.
- 10 See ESI† for further details.
- 11 The reaction does not reach 100% conversion during the time period in which kinetic data was recorded. This observation is easily understood when one considers that fact that the K_d for the [1a-2a] complex is 9.1 mM. Therefore, after the reaction has reached around 65% conversion, less than half of the remaining reagents are present as the reactive [1a-2a] complex. The overall rate of formation of 4a slows dramatically because the concentration of the reactive [1a-2a] complex drops rapidly above 65% conversion.
- 12 M. I. Page and W. P. Jencks, *Proc. Natl. Acad. Sci. U. S. A.*, 1971, **68**, 1678.
- 13 The kinetic effective molarity (kEM) is defined as the rate constant for the intracomplex reaction divided by the rate constant for the corresponding bimolecular reaction. The equilibrium or thermodynamic effective molarity (tEM) is defined as the equilibrium constant for the intracomplex reaction divided by the equilibrium constant for the corresponding bimolecular reaction. In practice, this can be derived from the kinetic data by expressing the equilibrium constant (K_{eq}) as a ratio of the rate constants for the appropriate forward and reverse processes ($k_{forward}/k_{reverse}$).
- 14 Using System II as the baseline system results in both System I and System III having apparently anomalous reactivity. It therefore seemed appropriate to apply Occam's Razor and assume that System II is the anomalous point in this data set.
- 15 (a) H. L. Rowe, D. Philp and N. Spencer, *Tetrahedron Lett.*, 2000, **41**, 4475; (b) R. M. Cowie, S. M. Turega and D. Philp, *Org. Lett.*, 2006, **8**, 5179.
- 16 (a) F. C. Lightstone and T. C. Bruice, *J. Am. Chem. Soc.*, 1996, **118**, 2595; (b) T. C. Bruice and F. C. Lightstone, *Acc. Chem. Res.*, 1999, **32**, 127.
- 17 (a) L. R. Domingo, M. J. Aurell, M. Arnó and J. A. Sáez, *J. Org. Chem.*, 2007, **72**, 4220; (b) L. R. Domingo, M. J. Aurell, M. Arnó and J. A. Sáez, *J. Mol. Struct.-Theochem.*, 2007, **811**, 125.
- 18 We define a Near Attack Conformation (NAC) for the dipolar cycloaddition as follows: the azide and the double bond of the maleimide to be aligned correctly with respect to each other and both of the two terminal nitrogen atoms of the azide must be located within 4.0 Å of the two carbon atoms of the alkene. Additionally, the hinge angle (see Table 2) must be within $\pm 15^\circ$ of the value calculated using DFT.
- 19 (a) P. Tecilla and A. D. Hamilton, *J. Chem. Soc., Chem. Commun.*, 1990, 1232; (b) P. Tecilla, V. Jubian and A. D. Hamilton, *Tetrahedron*, 1995, **51**, 435.
- 20 D. Hilvert, *Annu. Rev. Biochem.*, 2000, **69**, 751; For examples of cycloaddition reactions accelerated by catalytic antibodies see: (a) D. Hilvert, K. W. Hill, K. D. Nared and M-T. M. Auditor, *J. Am. Chem. Soc.*, 1989, **111**, 9261; (b) V. E. Gouverneur, K. N. Houk, B. Pascual-Teresa, B. Beno, K. D. Janda and R. A. Lerner, *Science*, 1993, **262**, 204; (c) A. C. Braisted and P. G. Schultz, *J. Am. Chem. Soc.*, 1990, **112**, 7430; (d) J. T. Yli-Kauhala, J. A. Ashley, C.-H. Lo, L. Tucker, M. M. Wolfe and K. D. Janda, *J. Am. Chem. Soc.*, 1995, **117**, 7041; (e) M. Resmini, A. A. P. Meekel and U. K. Pandit, *Pure Appl. Chem.*, 1996, **68**, 2025; (f) J. Xu, Q. Deng, J. Chen, K. N. Houk, J. Bartek, D. Hilvert and I. A. Wilson, *Science*, 1999, **286**, 2345.
- 21 COPASI 4.1 (Build 22). Copyright © 2005 by Pedro Mendes, Virginia Tech Intellectual Properties, Inc. and EML Research, gGmbH.
- 22 (a) M. W. Schmidt, K. K. Baldrige, J. A. Boatz, S. T. Elbert, M. S. Gordon, J. H. Jensen, S. Koseki, N. Matsunaga, K. A. Nguyen, S. Su, T. L. Windus, M. Dupuis and J. A. Montgomery, *J. Comput. Chem.*, 1993, **14**, 1347; (b) M. S. Gordon, M. W. Schmidt in *Theory and Applications of Computational Chemistry: the first forty years*, C. E. Dykstra, G. Frenking, K. S. Kim and G. E. Scuseria (Editors), Elsevier, Amsterdam, 2005, pp. 1167–1189.